Chemical pressure effect by selective deuteriation in the molecular-based conductor, 2,5-dimethyl-*N*,*N'*-dicyano-*p*-benzoquinone immine-copper salt, (DMe-DCNQI)$_2$Cu

Shuji Aonuma,* Hiroshi Sawa and Reizo Kato*

The Institute for Solid State Physics, The University of Tokyo, Roppongi, Minato-ku, Tokyo 106, Japan

The mixed-valence copper salt of DMe-DCNQI (**1**, where DMe-DCNQI = 2,5-dimethyl-*N*,*N'*-dicyano-*p*-benzoquinone diimine) is a molecular conductor whose electrical and magnetic properties are quite sensitive to pressure. We have performed selective deuteriation of the molecule **1**. By control of the position and number of deuterium atoms, the low-pressure region ($\lesssim$ 500 bar) † in the pressure–temperature phase diagram of (**1**)$_2$Cu was reproduced at ambient pressure. The equivalency of the deuteriation and pressure effects is explained from steric origins; 'contraction' aroused by the slightly shorter C–D bond (steric isotope effect) and 'constriction' by pressure.

DMe-DCNQI (**1**) is an organic π-acceptor first synthesized by Hünig and co-workers,[1,2] and forms many electroconductive salts with various inorganic metals.[3] Among them, the copper salt (**1-*h***)$_2$Cu is of special interest because an interaction between organic pπ electrons and inorganic d electrons has caused unique electrical and magnetic properties.[4,5]

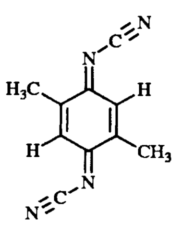

1-*h*

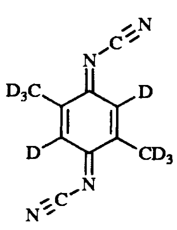

1-*d*$_8$

The crystal structure of the copper salt shows a one-dimensional stack of the molecule **1**. Moreover, the one-dimensional columns are linked by the copper ions through distorted tetrahedral coordination of the terminal nitrogen atoms of **1**.[2]

At ambient pressure, (**1-*h***)$_2$Cu remains in a metallic state down to the lowest temperature.[2] However, in contrast to most of the organic conductors in which the metallic state is stabilized by applying pressure, a sharp metal (M)–insulator (I) transition occurs above *ca.* 100 bar.[6] We call the former (metallic) behaviour type I and the later (M–I transition), type II. Replacement of the methyl groups with smaller substituents (Br, Cl) also simulates the application of pressure and results in the type-II behaviour.[2,5] Moreover, one of the most characteristic types of behaviour of this system is a novel M–I–M ('reentrant') transition (type III),[6] which is observed at the boundary between type-I and type-II regions. A schematic pressure–temperature phase diagram is shown in Fig. 1.

In the metallic state, the copper ion is in the mixed valence state (Cu$^{\sim 4/3+}$).[7] This indicates that the d electrons of the Cu ions are interacting with the organic pπ electrons near the Fermi level.[4,5] Recently, the de Haas–van Alphen effect measurement[8] has confirmed that this pπ–d interaction provides a three dimensional Fermi surface, which is the first case among the molecular-based conductors. The insulating state in the type-II region is accompanied by the charge density wave on the DCNQI column and the static charge ordering at the copper site ($\cdots \mathrm{Cu}^{2+}\mathrm{Cu}^{+}\mathrm{Cu}^{+} \cdots$), both of which have the three-fold periodicity along the stacking *c* axis.[4,9] It has been pointed out that the 3*c* period, in which the formal charge on the copper ion is exactly 4/3+, is energetically the most preferable.[10]

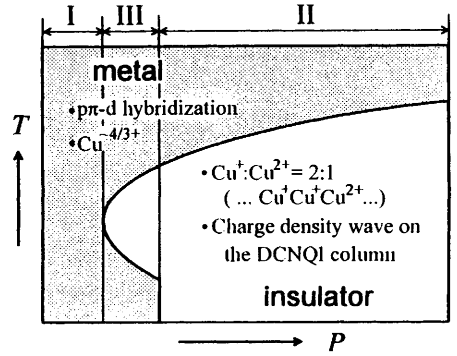

Fig. 1 Schematic pressure (*P*)–temperature (*T*) phase diagram of (R^1,R^2-DCNQI)$_2$Cu system. *P* includes 'chemical pressure' brought on by substituents or alloying effects.

The exotic electronic state of the present sytem, which drastically changes under pressure, has aroused keen interest. Under pressure, however, detailed investigations of this sytem had been hindered by technical difficulty. In addition, it is difficult to obtain single crystals of a large size and good quality in other DCNQI systems (including alloyed salts) except (**1**)$_2$Cu.

The discovery of the deuterium-induced M–I transition by Hünig *et al.*[11] brought a breakthrough to this situation. The electrical behaviour of the copper salts (**1-*d$_n$***)$_2$Cu (*n* = 3, 6, 8) reported by them[11a] corresponds to that in a pressure region of 250–500 bar. This remarkable isotope effect suggested to us that the effective pressure can be controlled by the number and position of deuterium atoms. Because the chemical difference

---

† 1 Bar = 10^5 Pa.

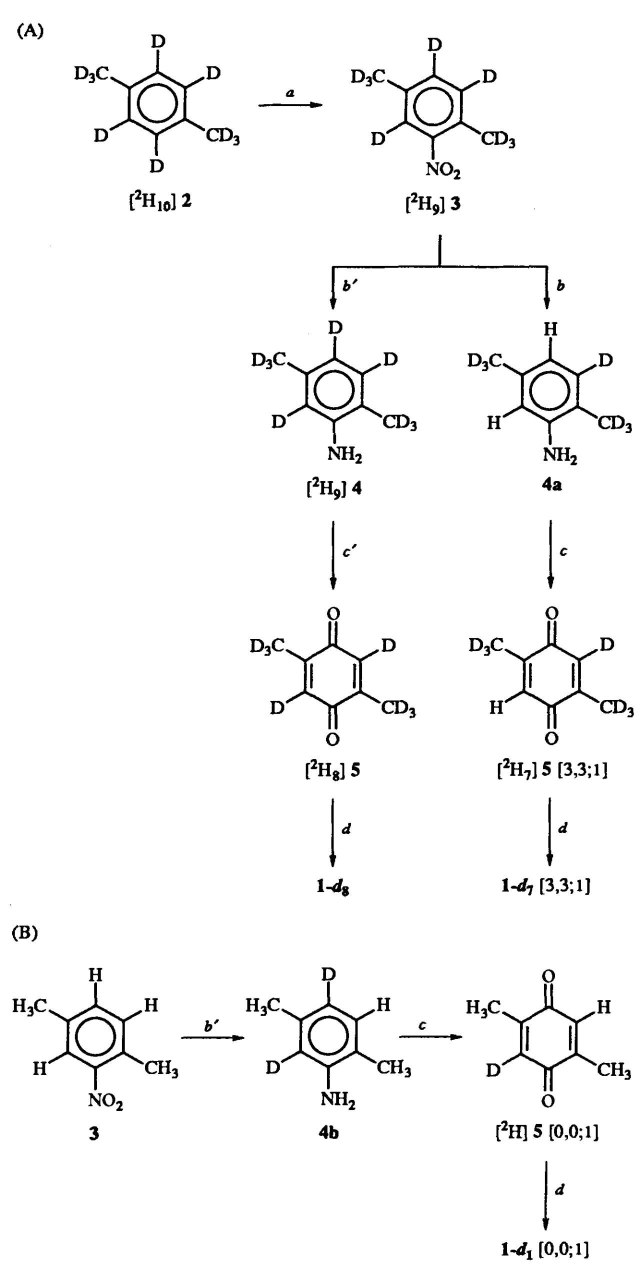

Scheme 1 Ring deuteriation. *a* HNO_3–H_2SO_4; *b* Zn in aq. HCl, *b′* in DCl; *c* $K_2Cr_2O_7$ in H_2SO_4, *c′* in D_2SO_4; *d* (1) $TiCl_4$, (2) $Me_3SiN{=}C{=}NSiMe_3$ in CH_2Cl_2.

between H and D atoms is almost negligible, the selective deuteriation promises that single crystals of a large size and good quality are available in all the regions (I, II and III) of the pressure–temperature phase diagram. In particular, we planned to reproduce the behaviour around the type-III region, where the drastic M–I–M transition occurs, by selective deuteriation.

The molecule **1** has 35 patterns of selective deuteriations for eight hydrogen sites. Mainly aiming at the type-III region, 15 deuterides are picked up among them. In this work, we have established the procedures for the selective deuteriation of **1** by combining several simple organic reactions. We describe herein their syntheses and electrical resistivities and discuss an orgin of the anomalous isotope effect.

Table 1 Correlation between reaction time and isotopic distribution of the H/D exchange reactions

	Isotopic distribution/D%[a]					
	[$^1H_9$]4			[$^2H_9$]4		
Reaction time	[$^1H_8$]	[$^2H_1$]	[$^2H_2$]	[$^2H_6$]	[$^2H_7$]	[$^2H_8$]
ca. 2 h	37	63	0	5	93	2
> 3 days	1	99	0	11	89	0

[a] Estimated from the mass spectra of the resultant **1-d_1[0,0;1]** and **1-d_7**[3,3;1].

Results and discussion

Synthesis

We had prepared **1-d_8**‡ from commercially available [$^2H_{10}$]*p*-xylene ([$^2H_{10}$]**2**) essentially according to the literature,[12] except that Zn in DCl–D_2O was used at the reduction step of the nitro group instead of D_2 gas and Pd–C [Scheme 1(A)]. This method is practically simpler, but isotopic purity does not exceed 95% probably due to the H/D exchange reaction during the work-up process for the 2,5-xylidine [$^2H_9$]**4**.

Ring deuteriations

When HCl was used isntead of DCl in Scheme 1(A), **1-d_7**[3,3;1] was obtained. This is mainly due to the *in situ* H/D exchange reaction of the fully-deuteriated 2,5-xylidine ([$^2H_9$] **4**).[13]

Similarly, when 2,5-xylidine ([$^1H_7$]**4**) was heated in DCl–D_2O, one ring deuterium atom per molecule was successfully introduced [Scheme 1(B)].

The exchange reaction from H to D proceeds more slowly and occurs more selectively at the positions *ortho* and *para* to the NH_2 group than that from D to H (Table 1). This difference may be ascribed to isotope effects on the bond break-up of the Wealand intermediate[14] and/or on the acid dissociation constant of HCl in H_2O against DCl in D_2O.

Even after heating 2,5-xylidine ([$^1H_7$]**4**) in DCl–D_2O for more than 3 days, introduction of a deuterium atom to the *meta* position was not detected by ^1H NMR spectroscopy. The introduction of one more deuterium atom requires much more extreme reaction conditions. All ring hydrogen atoms can be deuteriated by heating xylene in 50% D_2SO_4. The isotopic purity increased after several repetitions. As judged from ^1H NMR spectra, an exchange reaction at the methyl group does not occur under these conditions.

Methyl deuteriations

The most essential step is to obtain the methyl-deuteriated xylenes which can be ring deuteriated and converted to DMe-DCNQIs **1-d_n**. First, we prepared xylenes [^2H_n]**2** with $-CH_2D$, $-CHD_2$ or $-CD_3$ *via* deuterioreduction of carbonyl or chloromethyl groups,[15] which were then converted to the molecules **1-d_1**[1,0;0], **1-d_2**[2,0;0] and **1-d_3**[3,0;0], respectively. A similar reaction for *para*-substituted benzenes **6c** or **8e** afforded the xylene with two deuteriomethyl groups (**2e** or **2c**), respectively (Scheme 2). Thus, we can prepare any methyl-deuteriated xylenes by these methods. The reduction of chloride (step *h*) also proceeded using Zn and CH_3CO_2D in Et_2O.[16]

---

‡ We symbolically indicate deuteriated positions for the selective deuterides [^2H_n]**1** in the form of **1-d_n**[a_1,a_2; *b*], where a_1 and a_2 ($a_1 \geq a_2$) are numbers of deuterium atoms in each methyl group and *b* is that directly attached to the six-membered ring. Non- and fully-deuteriated **1** are represented as **1-*h*** and **1-d_8**, respectively. There exist two positional isomers for **1-d_2** [1,0;1]. They were used as a mixture in this work, because it requires additional steps to prepare them separately.

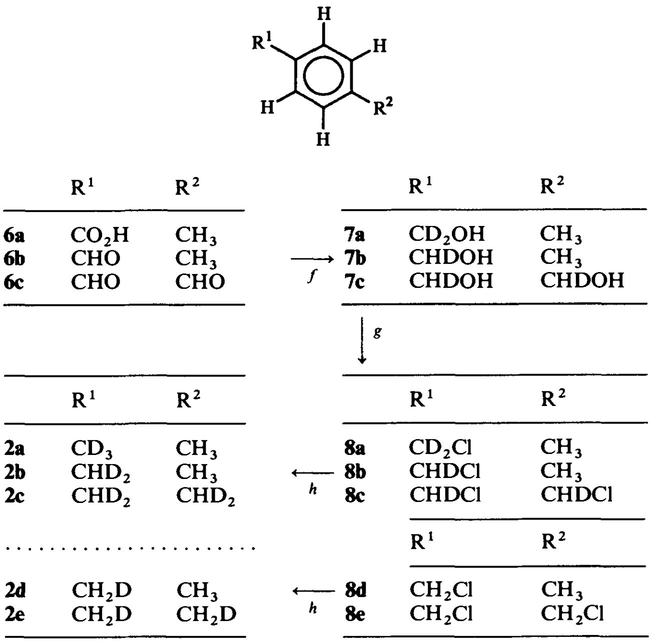

Scheme 2 Methyl deuteriation. *f* $LiAlD_4$ in Et_2O, *g* SO_2Cl, *h* $LiBEt_3D$ in THF.

Table 2 Synthetic routes for the quinone diimines **1-d_n** and isotopic purity (D%) estimated by mass spectroscopy

Starting material	Synth. step	Product	D%
2	*ab′c′d*	**1-d_1**[0,0;1]	99
2	*e′ab′c′d*	**1-d_2**[0,0;2]	96
8	*habcd*	**1-d_1**[1,0;0]	98
8	*h′abcd*	**1-d_1**[1,0;0]	94
8	*h′ab′c′d*	**1-d_2**[1,0;1][‡][i]	93
8	*h′e′ab′c′d*	**1-d_3**[1,0;2]	92
8e	*habcd*	**1-d_2**[1,1;0]	96
8e	*h′abcd*	**1-d_2**[1,1;0]	91
6b	*fghabcd*	**1-d_2**[2,0;0]	96
8e	*h′ab′c′d*	**1-d_3**[1,1;1]	90
8e	*h′e′ab′c′d*	**1-d_4**[1,1;2]	89
6a	*fghabcd*	**1-d_3**[3,0;0]	96
6a	*fghe′ab′c′d*	**1-d_5**[3,0;2]	95
6c	*fghabcd*	**1-d_4**[2,2;0]	90
$[^2H_{10}]$**2**	*eabcd*	**1-d_6**[3,3;0]	94
$[^2H_{10}]$**2**	*abcd*	**1-d_7**[3,3;1]	93
$[^2H_{10}]$**2**	*ab′c′d*	**1-d_8**	94

Steps: [a] Nitration of xylene. [b] Reduction of 2,5-dimethylnitrobenzene using Zn or $SnCl_2$ in HCl (*b*) or using Zn in DCl (*b′*). [c] Oxidation of xylidine to the quinone in H_2SO_4 (*c*) or in D_2SO_4 (*c′*). [d] Dicyanoimination of the quinone. [e] H/D exchange of xylene in H_2SO_4 (*e*) or in D_2SO_4 (*e′*). [f] Reduction of a carbonyl group. [g] Chlorination of benzyl alcohol. [h] Deuterioreduction of benzyl chloride using $LiBEt_3D$ (*h*) or Zn–CH_3CO_2D (*h′*). [i] Mixture of two positional isomers.

This method is preferable in terms of synthetic cost, but the isotopic purity is reduced to some extent. This is probably ascribed to insufficient exclusion of a radical impurity in reagents and/or media which promotes a radical side-reaction.

Combining the above mentioned methods, *i.e.* the ring deuteriation and the methyl deuteriation methods, the synthetic routes have been established for selective introduction of the deuterium atoms to desired positions. The deuterides synthesized herein, and their routes, are summarized in Table 2.

Spectral analysis

Isotopic purities of the molecules **1-d_n** were estimated by mass spectroscopy and the results are included in Table 2. The deuterium purity is also confirmed by the mass spectra of the precursor quinones **5** and NMR spectra of **1** and/or **5**.

^1H and ^{13}C NMR spectra also provide information on site specification of the deuterium atoms. Based on integral ratios and spin-coupling (H–D or ^{13}C–D) patterns, deuteriation site specificity within a molecule is confirmed. Deuteriation causes NMR chemical shifts to vary slightly and are explained as a normal isotope effect. Chemical shifts sometimes become a good probe for investigating the electronic nature of a molecule. In the present case, a remarkable difference was not observed.

The IR spectra of **1-d_n** also show normal isotopic shifts. The data for **1-d_8** are consistent with those previously reported.[12] A shift in the C–H stretching mode from 3040 to 2260 cm^{-1} (Table 5 in the Experimental section) is explained by the difference in mass (D/H $\simeq$ 2). There seems no extraordinary isotope effect upon the *intra*molecular vibration mode.

Complex formation

Physical properties of the $(1)_2Cu$ system are very sensitive to small amounts of impurities, especially monovalent metal such as Li, *e.g.* less than 1 mol% of Li stabilizes the metallic state.[17] Therefore, special precautions were taken for crystal growth. The copper salt crystals were prepared by the slow chemical reduction of **1** in the presence of $(Et_4N)_2[CuBr_4]$ by Bu_4NI in acetonitrile.[18] This method affords single crystals of sufficient quality for resistivity measurement and X-ray structural analysis within a single day.

Electrical resistivity

Electrical resistivity was measured by a conventional four-probe method. Because the electrical behaviour of this system is very sensitive to the sample or measurement conditions, we measured resistivity under as similar conditions as possible. As a result of prudent precautions, the observed transition temperature for samples in the same batches differs within a few degrees at most. The typical behaviour of electrical resistivity was exemplified in Fig. 2.

In Table 3 are listed the higher transition temperature T_1 and the lower transition temperature T_2 [for the type-III (reentrant) samples] in order of effective pressure (*vide infra*).

Each transition is accompanied by a hysteresis for the cooling and warming processes. The transitions for the type-II and type-III samples are extraordinarily sharp. Resistivity jumps or drops by several orders of magnitude within a temperature range of a few degrees.

Among the type-I (metallic) salts, the **1-d_1**[1,0;0] [Fig. 2(*b*)] and **1-d_2**[1,0;1] salts show a small anomaly around 40–50 K. The **1-d_3**[1,0;2] salt also shows a similar anomaly, but sometimes shows a sharp transition.

By just replacing the ring deuterium of **1-d_2**[1,0;1] by the methyl deuterium {the **1-d_2**[1,1;0] [Fig. 2(*c*)] or **1-d_2**-[2,0;0] salts}, the system completely enters the type-III (reentrant) region. These two d_2 salts show very similar behaviour. This suggests that the deuterium substitution pattern within the methyl groups is not significant. The other d_2 salts which possess no or a single methyl deuterium atom only indicate a small anomaly at low temperature. All these results indicate that methyl deuteriation is more effective than the ring deuteriation.

The salt on the borderline between the type-II and type-III regions would be the **1-d_3**[3,0;0] salt. Some samples in the same batch clearly indicate the reentrant transition, but the others do not.[§]

[§] Hünig and co-workers have also reported the **1-d_3**[3,0;0] salt, but made no mention of the reentrant transition.[11]

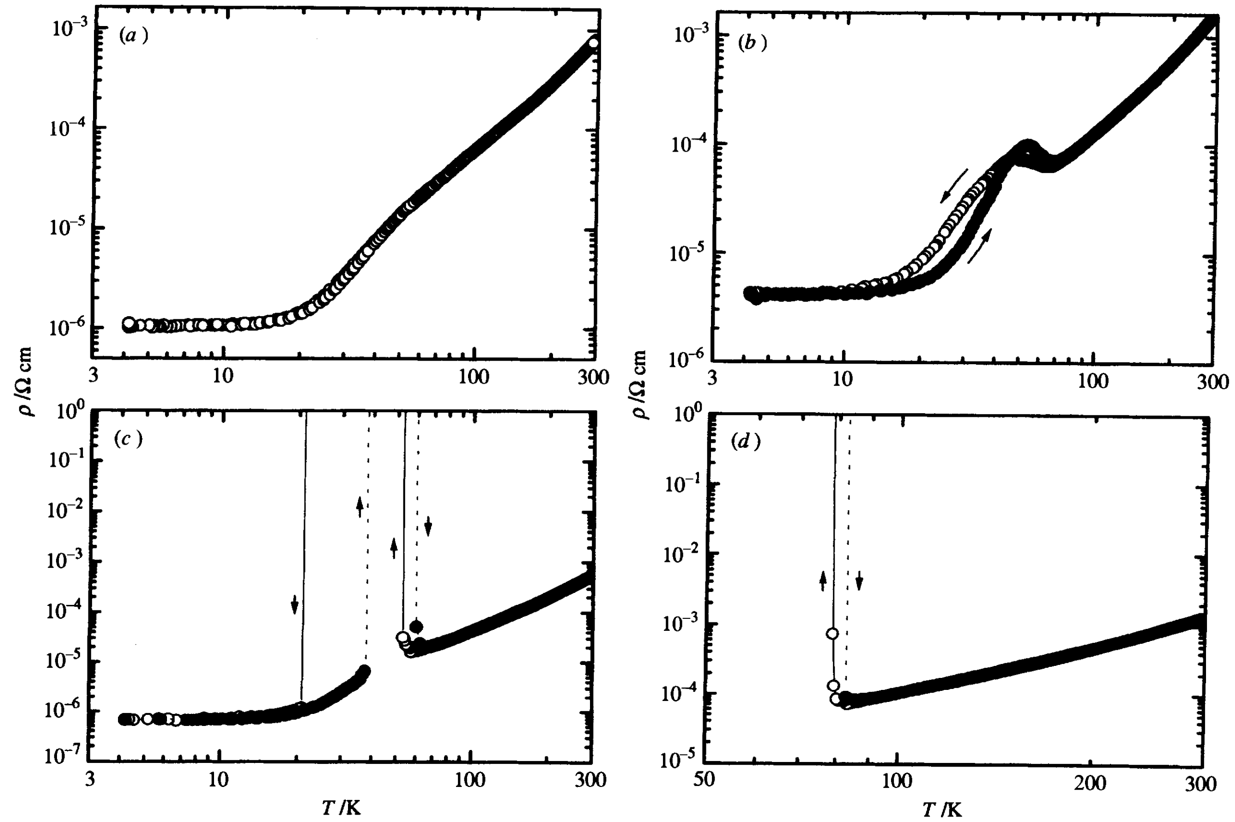

Fig. 2 Temperature dependence of electrical resistivity for (*a*) $(\mathbf{1}\text{-}\boldsymbol{h})_2\text{Cu}$, (*b*) $(\mathbf{1}\text{-}\boldsymbol{d}_1[1,0;0])_2\text{Cu}$ (type I), (*c*) $(\mathbf{1}\text{-}\boldsymbol{d}_2[1,1;0])_2\text{Cu}$ (type II) and (*d*) $(\mathbf{1}\text{-}\boldsymbol{d}_8)_2\text{Cu}$ (type III) samples. (*b*)–(*d*) –○– cooling; ··· ● ··· warming.

Table 3 Results of electrical resistivity measurements of $(\mathbf{1}\text{-}\boldsymbol{d}_n)_2\text{Cu}$

	Transition temperature				
	On cooling		On warming		
1-*d*$_n$	T_1	T_2	T_1	T_2	P_{eff}/bar[a]
1-*h*	*b*	*b*	*b*	*b*	(0)
1-*d*$_1$[0,0;1]	*b*	*b*	*b*	*b*	16
1-*d*$_2$[0,0;2]	*ca.* 40 (slight sh)[c]		*ca.* 50 (slight sh)[c]		32
1-*d*$_1$[1,0;0]	*ca.* 40 (sh)[c]		*ca.* 50 (sh)[c]		80
1-*d*$_2$[1,0;1]	*ca.* 40 (sh)[c]		*ca.* 50 (sh)[c]		96
1-*d*$_3$[1,0;2][d]	51	28	54	41	112
1-*d*$_2$[1,1;0]	55	21	56	35	160
1-*d*$_2$[2,0;0]	55	20	58	35	160
1-*d*$_3$[1,1;1]	57	16	63	30	176
1-*d*$_4$[1,1;2]	61	13	59	33	192
1-*d*$_3$[3,0;0][e]	62	10	66	22	240
	64	*b*	67	*b*	
1-*d*$_5$[3,0;2]	66	*b*	70	*b*	272
1-*d*$_4$[2,2;0]	68	*b*	71	*b*	320
1-*d*$_6$[3,3;0]	75	*b*	78	*b*	480
1-*d*$_7$[3,3;1]	77	*b*	80	*b*	496
1-*d*$_8$	80	*b*	82	*b*	512

[a] Calculated from $P_{\text{eff}} \simeq 80\,(a_1 + a_2 + 0.2b)$ (see text). [b] Transition is not observed. [c] sh stands for shoulder. Some samples do not indicate any anomaly. [d] Some samples indicate no sharp reentrant transition, but only a shoulder at *ca.* 50 K. [e] Some samples do not indicate the reentrant transition.

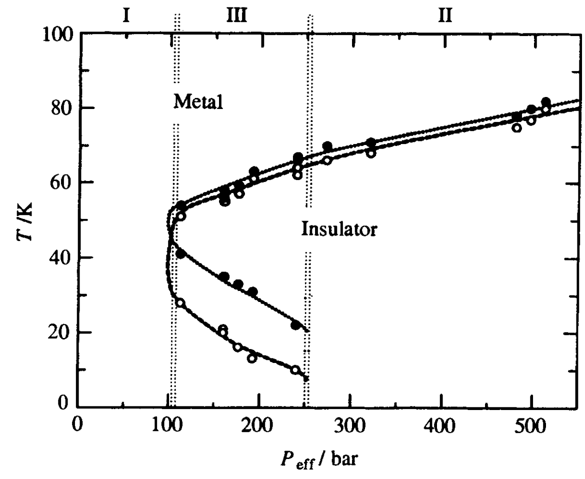

Fig. 3 Effective pressure (P_{eff}) *vs.* temperature (*T*) phase diagram of the $(\mathbf{1}\text{-}\boldsymbol{d}_n[a_1,a_2;b])_2\text{Cu}$ system obtained by using the equation $P_{\text{eff}} \simeq 80\,(a_1 + a_2 + 0.2b)$. ○ Cooling; ● warming.

Owing to the similarity between the effect of pressure and of deuterium atoms, the transition temperatures listed in Table 3 were compared with those under pressure.[6] The effective pressure (P_{eff}) is consequently formulated as eqn. (1). The P_{eff}–*T* phase diagram (Fig. 3) reproduces the low pressure ($\lesssim 500$ bar) region of the *P*–*T* phase diagram for $(\mathbf{1})_2\text{Cu}$.[6]

$$P_{\text{eff}} = 80\,(a_1 + a_2 + 0.2b) \qquad (1)$$

Crystal structure

A series of **1-*d*$_n$** salts are all isostructural with the space group $I4_1/a$. To detect structural differences between these deuterides, X-ray single-crystal structure analysis was applied at room temperature. Any change in the structural features (the coordination geometry, intermolecular distances *etc.*) upon the

Table 4 Lattice constants of $(\mathbf{1}\text{-}d_n)_2$Cu with standard deviations at room temperature

	a/Å	c/Å	V/Å^3
1-h	21.611(2)	3.8783(6)	1811.2(4)
1-d_1[1,0;0]	21.6068(11)	3.8787(6)	1810.8(3)
1-d_2[1,1;0]	21.6078(8)	3.8771(6)	1810.2(3)
1-d_3[1,1;1]	21.6071(17)	3.8757(5)	1809.5(3)
1-d_4[1,1;2]	21.6025(17)	3.8770(4)	1809.3(4)
1-d_7[3,3;1]	21.6027(14)	3.8754(4)	1808.6(3)
1-d_8	21.607(2)	3.8741(7)	1808.7(5)

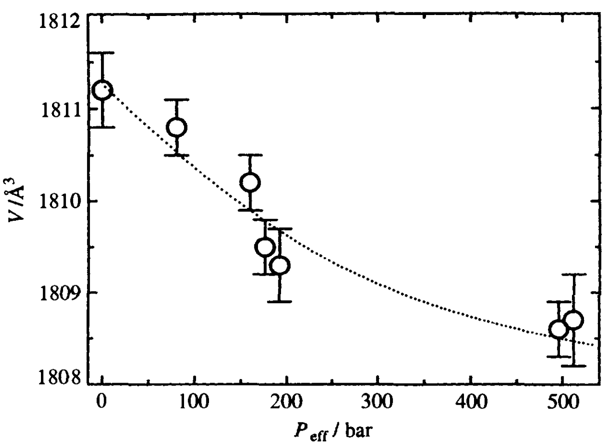

Fig. 4 Correlation between effective pressure (P_{eff}) and cell volume (V). The dotted line is a guide for the eyes.

deuteriation could not be detected within the accuracy of the X-ray structure analysis.[13] So, we performed accurate analysis of the lattice constants using a fine-focus filament for non-monochromated Mo-Kα_1 radiation, which have revealed slight, but obvious contraction of the unit cell by deuteriation (Table 4). Correlation between the cell volume (V) and the effective pressure (P_{eff}) is shown in Fig. 4.

Origin of the isotope effect

Let us consider the origin of the drastic isotope effect. The present case is classified as a secondary isotope effect, where no bond-beaking occurs. In most cases, the secondary effect is much smaller than the primary one and only its physical property varies quantitatively. However, the drastic qualitative change (M–I transition) is relevant to the present case.

Considering the contraction of the unit cell by deuteriation, the most plausible origin of the isotope effect[11,13,19] upon $(\mathbf{1})_2$Cu is the steric isotope effect.[20] A C–D bond is slightly shorter than a C–H bond[21] because of the lower zero-point energy. Owing to the steric isotope effect, each DCNQI molecule becomes a bit less bulky by deuteriation and they come closer to each other. This situation is quite similar to that under pressure. In this sense, the deuteriation is considered equivalent to the application of pressure. Although it was not clear until now how the application of pressure causes the M–I transition, the distortion of the coordination tetrahedron around the copper is believed to play an important role.[17]

It is difficult to evaluate the adequacy of the pressure effect of 500 bar brought in by the perdeuteriation. However, it is worth noting that perdeuteriation of nitromethane corresponds to applying *ca.* 400 bar of pressure.[22] It is almost the same value as that in the present case, although the molecular environment is not similar.

The effectiveness of the methyl deuterium atom compared with the ring one can be illustrated from the structure of the one-dimensional column formed by DCNQI molecules **1**, where the adjacent methyl groups are close to each other and therefore the intermolecular distance is mainly affected by repulsions between the methyl groups [Fig. 5(*a*)].[19]

The ring deuterium atom possesses a much smaller, but certain effect. This can be explained from the rather short distance between the ring hydrogen and the terminal cyano nitrogen of the neighbouring molecule [Fig. 5(*b*)].

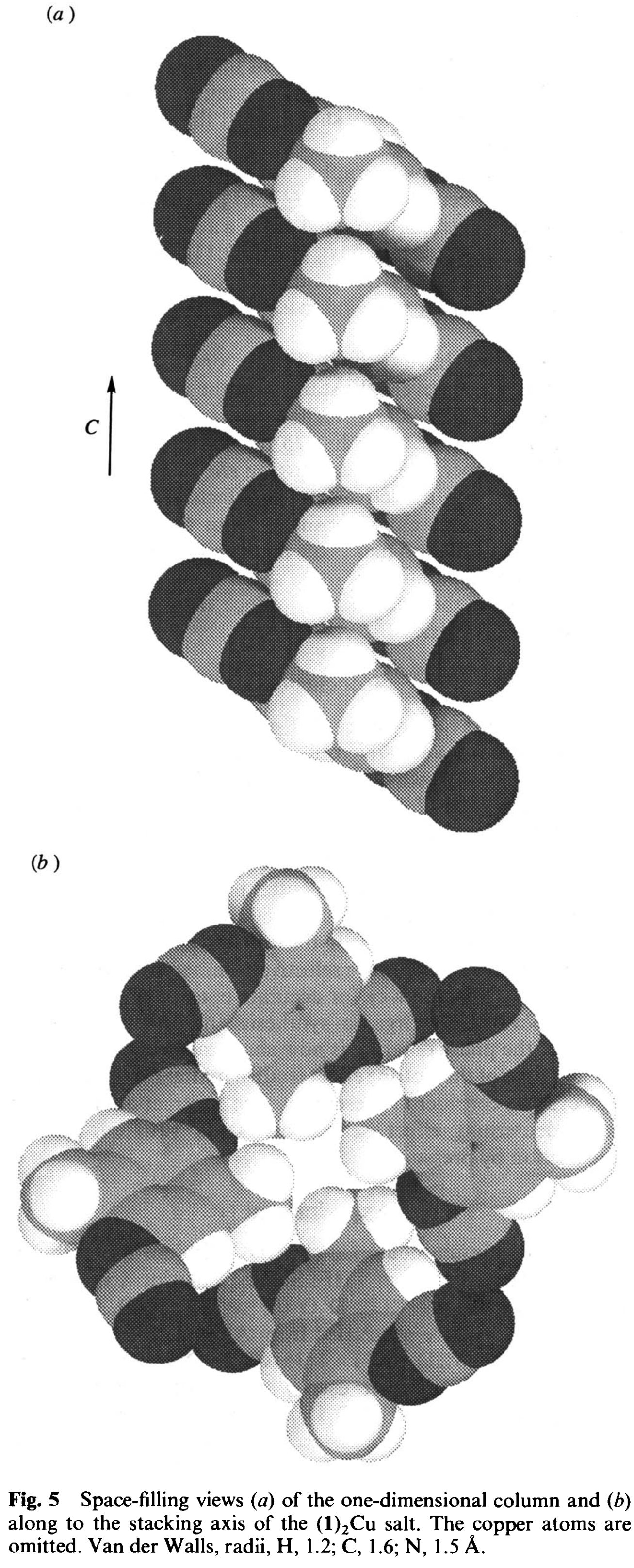

Fig. 5 Space-filling views (*a*) of the one-dimensional column and (*b*) along to the stacking axis of the $(\mathbf{1})_2$Cu salt. The copper atoms are omitted. Van der Walls, radii, H, 1.2; C, 1.6; N, 1.5 Å.

The steric isotope effect is the most plausible explanation, however, there remains another possibility. This is the inductive isotope effect.[23] A slight difference in the electron affinities of H and D might reflect upon the reduction potentials. This inductive isotope effect may slightly shift the charge (q) on the DCNQI molecule. By means of cyclic voltammetry and differential pulse polarography, no difference in the redox potentials between **1-*h*** and **1-*d*$_7$**[3,3;1][13] or **1-*d*$_8$** could be detected. However, as estimated from a recent experiment of charge-transfer control for (**1-*d*$_7$**[3,3;1])$_2$Cu by lithium doping,[17] the pressure effect induced by one methyl deuterium (δP = 80 bar) may correspond to a charge change of only $\delta q = -0.003$.

Recently, we have proposed that one of the essential parameters which govern the stability of the metallic state is the amount of charge-transfer from the copper to the DCNQI.[17] This parameter is variable according to the coordination geometry around the copper, the lithium doping *etc.* In our model, both the steric and the inductive isotope effects lead to the same situation, *i.e.* extra charge transfer from the copper to the DCNQI. This situation makes the metallic state less stable.[17] In any case, it is apparent that quite small changes in the crystal associated with the deuteration induce drastic variations in the physical properties.

Conclusions

The low pressure region of the P–T phase diagram of the (**1**)$_2$Cu salt was formerly accessible only by means of the helium gas pressure method,[6] which requires special apparatus and a skillful technique for accurate measurements. This has prevented a detailed investigation of the chemistry and physics of this sytem, especially the type-III (M–I–M transition) region. We found that one methyl deuterium atom per molecule corresponds to a pressure of *ca.* 80 bar and that the ring deuterium is about a fifth of the methyl one. We have also established how to introduce selectively deuterium atoms to the molecule **1**. Thus, the way for accurate control of 'pressure' is now achievable by organic synthesis and the low-pressure region of the phase diagram is now chemically reproduced.

The origin of the isotope effect is still a matter for speculation. However we consider at present that the contraction due to the steric deuterium effect serves the same situation as the constriction by pressure.

Experimental

Lithium aluminium deuteride ($LiAlD_4$), lithium triethylborodeuteride (1 mol dm^{-3} in THF; Super-Deuteride®, $LiEt_3BD$), [$^2H_{10}$]*p*-xylene (>99%D), D_2O (65 wt% in D_2O, 99.9%D), DNO_3 (98%D) were purchased from Aldrich, and D_2SO_4 (96 wt% in D_2O, 99.3%D) and DCl (35 wt% in D_2O, 99.9%D) were from ISOTEC. They were used without further purification. [*O*-^{2}H]Acetic acid (CH_3CO_2D) was prepared and distilled according to a literature method[16] from D_2O and acetyl chloride. The acetyl chloride was distilled in the presence of *N*,*N*-dimethylaniline.

In order to avoid isotopic contamination caused by moisture in the air, deuterides were carefully handled, weighed and transferred under sufficient flow of argon gas. The reaction in which deuterides were used was carried out under an argon atmosphere in the apparatus which was repeatedly evacuated (whilst being heated by a heat gun if possible) and flushed with argon to the complete exclusion of moisture. Diethyl ether and tetrahydrofuran (THF) were distilled over sodium benzophenone ketyl under argon just before use. Acetonitrile was repeatedly distilled from phosphorus pentoxide under argon.

NMR spectra were recorded on a JEOL JNM-EX90 FT (90 MHz for ^{1}H and 22.5 MHz for ^{13}C) or on a JEOL JNM-PMX60SI CW (60 MHz for ^{1}H) NMR spectrometer in $CDCl_3$, unless otherwise noted, at room temperature with tetramethylsilane as the internal standard. ^{1}H FT-NMR spectra taken with a sufficiently high signal-to-noise ratio was used for estimation of isotopic purity. The data of the ^{13}C NMR spectra listed here were of the complete decoupling ($^{13}C\{^1H\}$) method, and s (singlet), t (triplet), quintet and septet are ascribed to ^{13}C–D spin couplings. J values are given in Hz. In order to confirm the assignment, DEPT (distortionless enhanced polarization transfer) spectra were taken in some cases. IR spectra were run as KBr discs using a Hitachi–Nicolet I-5040 FT-IR spectrometer at a resolution of 2 cm^{-1} at room temperature. Mass spectra were taken on a JEOL JMS-QH100 or on a JEOL JMS-AX500 spectrometer (EI, 70 eV).

Reduction of the carbonyl group to a hydroxymethyl group (step *f*)

Over a 2 h period, *p*-tolualdehyde **6b** (58.7 g, 0.489 mol) was added dropwise to a stirred suspension of $LiAlD_4$ (6.1 g, 0.145 mol) in dry diethyl ether (250 cm^3). After the resultant greyish suspension was refluxed overnight, water (6 cm^3), 15% aq. NaOH (18 cm^3) and water (6 cm^3) were added successively with care at room temperature. The gummy white precipitation was filtered and extracted with diethyl ether. The concentration of the ether extract afforded [α-^{2}H]-4-methylbenzyl alcohol **7b** (59.3 g, 0.482 mol, 99%) as white needles; δ_H(90 MHz) 2.32 (s, CH_3 and OH), 4.53 (br s), 7.11 (d, J^3_{HH} 8.6) and 7.21 (d, J^3_{HH} 8.6), 99% D. The chemical shift of the alcohol hydrogen depended on the measurement conditions such as concentration.

Similar treatment of methyl 4-methylbenzoate (**6a**) with $LiAlD_4$ in THF refluxed for over 60 h yielded [α,α-$^2H_2$]-4-methylbenzyl alcohol **7a** in a quantitative yield; δ_H(90 MHz) 1.83 (s, OH), 2.34 (s), 7.11 (d, J^3_{HH} 8.3) and 7.21 (d, J^3_{HH} 8.3), ≃ 100% D.

Also [α,α′-$^2H_2$]benzene-1,4-dimethanol **7c** (74%) was obtained from the reaction of $LiAlD_4$ and terephthalaldehyde **6c** in diethyl ether by refluxing over 5.5 days.

Chlorination of OH using thionyl chloride (step *g*)

To the alcohol **7b** (58.9 g, 0.478 mol) was added thionyl chloride (47 cm^3) under argon. After the addition was over (40 min), pyridine (*ca.* 0.2 cm^3) was added. After being heated at 80 °C for 2 h, the mixture was poured into ice–water (1 dm^3) and extracted with diethyl ether. The ether extract was washed with 5% HCl, dried ($MgSO_4$), and evaporated *in vacuo* to afford [α-^{2}H]-4-methylbenzyl chloride **8b**; δ_H(90 MHz) 2.31 (s), 4.74 (t, J^2_{HD} 1.7), 7.09 (d, J^3_{HH} 8.5) and 7.23 (d, J^3_{HH} 8.5).

The isotopic purity estimated from the integral ratio erroneously exceeds 100%.

In a similar way, **7a** afforded [α,α-$^2H_2$]-4-methylbenzyl chloride **8a** (99%); δ_H(90 MHz) 2.21 (s), 7.00 (d, J^3_{HH} 8.1) and 7.14 (d, J^3_{HH} 8.1), 98% D.

The diol **7c** afforded [α,α′-$^2H_2$]benzene-1,4-bis(chloromethane) **8c** (97%); δ_H(90 MHz) 4.57 (t, CHDCl, J^2_{HD} 1.8) and 7.39 (s).

Reduction of α-chloromethyl group (step *h*)

Using $LiBEt_3D$ in THF (*h*). To the chloride **8b** (18.4 g, 0.129 mol), 1 mol dm^{-3} THF solution of Super-Deuteride (205 cm^3) was added dropwise for 1.5 h with cooling with an ice–water bath. After being stirred for 16 h, D_2O (4 cm^3) was carefully added for 3 min. Then, 3 mol dm^{-3} NaOH (120 cm^3) and 31% H_2O_2 (120 cm^3) were added successively. The reaction mixture was extracted with diethyl ether. The extracts were washed with 50% sulfuric acid and dried ($MgSO_4$). After passing through a short silica gel column, evaporating the diethyl ether by a rotary evaporator, distillation at ambient pressure afforded [α,α-$^2H_2$]*p*-xylene **2b** (8.7 g, 0.080 mmol, 62%); δ_H(90 MHz) 2.27 (s + t) and 7.02 (s), 96%D.

Similarly [α-^{2}H]*p*-xylene **2d** (85%) was obtained from 4-methylbenzyl chloride **8d**; δ_H(90 MHz) 2.30 (s), 2.29 (t, J^2_{HD} *ca.* 2) and 7.06 (s); δ_C(22.5 MHz) 20.6 (t, J^1_{CD} 19.3), 20.9 (s), 128.9 (s) and 134.7 (s).

Reaction of benzene-1,4-bis(chloromethane) **8e** with 1.6 equiv. of Super-Deuteride afforded [α,α′-$^2H_2$]*p*-xylene **2e** (79%); δ_H(90 MHz) 2.26 (t, J^2_{HD} 2.1) and 7.02 (s), 99%D; δ_C(22.5 MHz) 20.6 (t, J^1_{CD} 19.3), 128.9 (s) and 134.6 (s).

The chloride **8a** afforded [α,α,α-$^2H_3$]*p*-xylene **2a** (65%); δ_H(90 MHz) 2.30 (s) and 7.06 (s), 99%D.

Similarly, [α,α,α′,α′-2H_4]*p*-xylene **2c** (58%) was obtained from the dichloride **8c**; δ_H(90 MHz) 2.26 (quint., CHD_2, J^2_{HD} 2.2) and 7.05 (s).

Using Zn in CH_3CO_2D (*h*′). To a suspension of fine zinc powder (13.4 g, 0.204 mol) in CH_3CO_2D (20 cm^3, *ca.* 0.35 mol) and diethyl ether (200 cm^3) cooled to 2–4 °C by means of an ice–water bath, a 100 cm^3 diethyl ether solution of the chloride **8d** (15.5 g, 0.110 mol) was added for 2 h. The reaction mixture was stirred overnight at room temperature. Then, water (200 cm^3) was added, the organic layer was separated and the aqueous layer was extracted with diethyl ether. The combined organic layer was washed with 10% Na_2CO_3 and water, dried and distilled (bp 136.5 °C) to yield [α-^{2}H]*p*-xylene **2d** (9.24 g, 0.0862 mol, 78%); δ_H(90 MHz) 2.28 (s + t) and 7.05 (s).

[α,α′-$^2H_2$]*p*-Xylene **2e** (80%) was obtained from benzene-1,4-bis(chloromethane) **8e**; δ_H(90 MHz) 2.31 (t, J^2_{HD} 2.1) and 7.08 (s), 98%D.

H/D exchange reaction of xylene

In D_2SO_4 (step *e*). A mixture of *p*-xylene **2** (27 g), D_2O (30 cm^3) and D_2SO_4 (31 cm^3) was heated at 110 °C for 2 days and the organic layer was separated (77%D; estimated from ^{1}H NMR spectroscopy). Further treatments of this xylene with D_2O (15 cm^3) and D_2SO_4 (15 cm^3) for 22 h (96%D), then D_2O (20 cm^3) and D_2SO_4 (20 cm^3) for 15 h afforded [2,3,5,6-$^2H_4$]*p*-xylene (~99%D).

The deuterides [2,3,5,6,α-$^2H_5$]*p*-xylene, [2,3,5,6,α,α′-$^2H_6$]*p*-xylene and [2,3,5,6,α,α,α-$^2H_7$]*p*-xylene were prepared in a similar way.

In H_2SO_4 (step *e*′). Similar repetitions (5 × 6 days) of the exchange reaction of [$^2H_{10}$]*p*-xylene ([$^2H_{10}$]**2**) (10 g) in H_2SO_4 (17 cm^3) and H_2O (20 cm^3) afforded [α,α,α,α′,α′,α′-$^2H_6$]*p*-xylene (**2f**).

Nitration of xylene (step *a*)[12,24]

To perdeuteriated xylene ([$^2H_{10}$]**2**) (20 g, 0.17 mol), a mixture of DNO_3 (25 g) and D_2SO_4 (28 cm^3) was added dropwise over 70 min carefully keeping the temperature of the reaction mixture below 20 °C by cooling in an ice–water bath. After being stirred for an additional 4 h at room temperature, the reaction mixture was poured onto ice (125 g) and extracted with diethyl ether. The extract was washed with 10% Na_2CO_3 and dried ($MgSO_4$). After the diethyl ether was distilled off at ambient pressure, [$^2H_9$]2,5-dimethylnitrobenzene ([$^2H_9$]**3**) (15.6 g, 56%) was distilled as a pale yellow liquid (bp 135–145 °C/*ca.* 38 mmHg); δ_H(90 MHz; neat) 2.25 (quintet, J^2_{HD} 2.3), 2.38 (quintet, J^2_{HD} 2.2), 7.06 (br s), 7.17 (br s) and 7.58 (s); δ_C(22.5 MHz) 18.0 (septet, J^1_{CD} 19.7), 18.5 (septet, J^1_{CD} 19.4), 123.5 (t, J^1_{CD} 27.4), 129.3 (s), 131.3 (t, J^1_{CD} 24.7), 132.6 (t, J^1_{CD} 24.3), 136.1 (s) and 148.1 (s).

For preparations of other deuteriated 2,5-dimethylnitrobenzenes, H_2SO_4 and HNO_3 were used instead and their yields were 72–90%. Because this reaction proceeds at a rather low temperature (below 20 °C), a loss of isotopic purity by the H/D exchange reaction was not observed.

Reduction of nitroxylene using Zn or $SnCl_2$

In HCl with Zn or $SnCl_2$ (step *b*). Tin(II) dichloride dihydrate (34.3 g, 0.152 mol) in conc. hydrochloric acid (22.5 g) was added dropwise to [$^2H_9$]**3** (4.86 g, 0.0303 mol) at a rate at which the temperature was kept below 60 °C. After the addition was over (50 min) the reaction mixture was heated at 90 °C for 2 h, then cooled to room temperature, poured into ice-cooled 50% aq. NaOH (1 dm^3) and extracted with diethyl ether. The extract was washed with 10% aq. NaCl, dried (Na_2CO_3) and distilled to yield [3,α,α,α,α′,α′,α′-$^2H_7$]-2,5-dimethylaniline (**4a**) (81%); bp 121–122 °C/37 mmHg.

In DCl with Zn (step *b*′). To a vigorously stirred mixture of fine zinc powder (27.8 g, 0.426 mol), perdeuteriated 2,5-dimethylnitrobenzene [$^2H_9$]**3** (15.4 g, 0.0961 mol) and D_2O (83 cm^3), DCl (100 g) was added dropwise over 45 min at a rate such that the temperature did not exceed 90 °C. After being stirred for 2 h, the reaction mixture was poured into ice-cooled 30% aq. NaOH (900 cm^3) and extracted with diethyl ether. The extract was washed with 10% NaCl and dried (Na_2CO_3). The diethyl ether was distilled off at ambient pressure and [$^2H_9$]2,5-dimethylaniline [$^2H_9$]**4** (9.27 g, 74%) was given (bp 119–124 °C/38 mmHg). The deuteriated amino group ($-ND_2$) was exposed to H/D exchange during the work-up and was converted to $-NH_2$.

[3,4,6,α,α′-$^2H_5$]2,5-Xylidine (73%) was obtained in a similar way.

Oxidation of xylidine to 2,5-dimethylbenzo-1,4-quinone (step *c*)

A mixture of D_2O (270 cm^3) and D_2SO_4 (42 cm^3) was cooled to 5 °C and perdeuteriated xylidine ([$^2H_9$]**4**) (9.22 g, 0.0708 mol) was added. Then $K_2Cr_2O_7$ (11.0 g, 0.0374 mol) was added for 5 min. After being stirred and warmed from 5 °C to room temperature for 16 h, the reaction mixture was cooled in an ice–water bath again. Further $K_2Cr_2O_7$ (23.3 g, 0.0758 mol) was added for 3 min. After being stirred for 17 h at room temperature, the mixture was extracted with CH_2Cl_2. The extract was washed with 10% NaCl and dried ($MgSO_4$). The solvent was removed and the residue was chromatographed over a silica gel column by using CH_2Cl_2 as eluent to yield a yellow powder (5.72 g) which recrystallized from methanol to afford [$^2H_8$]2,5-dimethylbenzo-1,4-quinone ([$^2H_8$]**5**) (3.66 g, 36%) as bright yellow crystals; δ_C(22.5 MHz) 14.4 (septet, J^1_{CD} 19.7), 132.8 (t, J^1_{CD} 25.2), 145.3 (s) and 187.8 (s).

Cyanoimination of the quinone (step *d*)[1]

To a CH_2Cl_2 (70 cm^3) solution of perdeuteriated quinone [$^2H_8$]**5** (1.44 g, 0.0100 mol) under argon, a CH_2Cl_2 (20 cm^3) solution of $TiCl_4$ (6.2 g, 0.033 mol) was added for 5 min and then a CH_2Cl_2 (10 cm^3) solution of bis(trimethylsilyl)-carbodiimide (6.3 g, 0.034 mol) was added. After being stirred for 4 h at room temperature the reaction mixture was poured into ice–water (1 dm^3) and extracted with CH_2Cl_2. The combined extract was washed with water, dried ($MgSO_4$) and concentrated to saturation on a rotary evaporator. Addition of petroleum ether (500 cm^3) caused immediate formation of yellow microcrystals which were recrystallized twice from hot acetonitrile to yield DMe-DCNQI **1-*d*$_8$** (1.09 g, 0.005 69 mol, 57%) as bright orange plates. IR data are shown in Table 5.

Crystal preparation

In the Schlenk tube with a two-way stopcock and a dropping funnel, **1-*d*$_n$** (40 mg, 0.21 mmol) and ($Et_4N_2[CuBr_4]$ (70 mg, 0.11 mmol) were placed under an argon atmosphere. Acetonitrile (40 cm^3) was transferred to the funnel and added to the flask after bubbling with dry argon gas. Then the flask was immersed in ultrasonic waves until the crystals were completely dissolved. Then, tetrabutylammonium iodide (50 mg, 0.14 mmol) was added at once under an argon flush and quickly dissolved. The black needles (15 mg) were formed on standing at 20.0 °C in the dark over a day. All apparatus should be very

Table 5 IR absorptions (cm^{-1}) of **1**-d_n (KBr disc)

1-h	**1**-d_1[0,0;1]	**1**-d_2[0,0;2]	**1**-d_1[1,0;0]	**1**-d_3[1,0;2]	**1**-d_2[1,1;0]	**1**-d_4[1,1;2]	**1**-d_7[3,3;1]	**1**-d_8	
3041w			3040w		3034sh		3041w		ν_{CH}
3019w	3020w	3015w	3021w	3014w	3021w	3013w	3018w	3014w	
3000w	2991vw		2999w		2995w		3000vw		
	2260w	2256w		2268w		2262w	2263w	2264w	ν_{CD}
				2253w			2251w		
2188sh			2184sh					2181sh	
2178sh			2175vs	2172vs	2182vs	2174vs	2178vs	2172vs	ν_{CN}
2167vs	2175vs	2174vs	2165sh		2170sh				
1592s	1585s	1579s	1591s	1577s	1591s	1576s	1578s	1571s	$\nu_{C=C}$
1546sh	1545sh	1542sh	1546sh	1542sh	1546sh	1541sh	1543sh	1544sh	
1537vs	1536vs	1532vs	1537vs	1532vs	1537vs	1531vs	1534vs	1532vs	$\nu_{C=N}$
1425w	1426w	1425w	1423w	1420w	1426w	1420w		1421w	
1378s	1382s	1380s	1374s	1373s	1373w	1373vw	1363vw	1358vw	
	1361m	1343m		1343m		1346m	1336vw	1341w	
1284s	1288m		1287m	1281w	1290w	1283w	1282m		
	1278sh		1276m		1280m				
	1266sh		1265m	1263m	1266m	1265m			
1182m	1195m	1266m	1178m	1211m	1173w	1198w	1194s	1209s	
1169m	1188sh		1165m		1153w				
			1158m						
1052m			1050m	1049vw	1047m				
1038m	1038m	1032w	1038	1029vw		1034vw	1033m	1034m	
1002m	1000m	1002m	991m	994m	991m			993m	
	960w	967m	925m	965m	925s				
911s	898s		911s		909m		934m		
			904sh	880vw	899m	883vw			
838m	802m		841m	834m			846m	821w	
			805w	803w					
	788s	770s		771s		771s		771s	
	706s						753w	741w	
687w	684m	681	680m	676m	676m	670w	704m		
	668vw		639sh		631m				
643m	626w	623w	634m	611vw	624m		650w	647w	
566m	559m	544m	565m	553m	564m	555m	556w	554w	
422s	404s		420s		417s				

clean, because the electrical properties of the crystals can be affected by a trace of contaminant, especially lithium ions.

Electrical resistivity

Electrical resistivity (ρ) was measured along the crystallographic c axis (needle axis) by the standard DC four-probe method down to 4.2 K. Electrical contacts were made with conductive carbon paste using 10 μm gold wires.

Single crystal structure analysis

Intensity data were collected on a MAC science automatic four-circle diffractometer with monochromatized Mo-Kα radiation up to $2\theta = 60°$ at room temperature. The structures were determined by the direct method and refined by the full-matrix least-squares method.

Lattice constants

Lattice constants were determined by least-squares refinement for 24 reflections with $39° < 2\theta < 47°$ measured on the MAC Science automated four-circle diffractometer at room temperature. In order to gain the best accuracy, we used non-monochromated Mo-Kα_1 radiation with a fine focus filament (0.3 × 3 mm).

Acknowledgements

We are grateful to Professor Minoru Kinoshita and Mr Masafumi Tamura for the use of an FTIR spectrometer. This work was partially supported by a Grant-in-Aid for Scientific Research on Priority Area 'Molecular Magnetism' (Area No. 288/04242103) from the Ministry of Education, Science and Culture, Japan.

References

1 A. Aumülar and S. Hünig, *Liebigs Ann. Chem.*, 1986, 142.
2 (*a*) A. Aumüller, P. Erk, G. Klebe, S. Hünig, J. U. von Schütz and H.-P. Werner, *Angew. Chem., Int. Ed. Engl.*, 1986, **25**, 740; (*b*) S. Hünig and P. Erk, *Adv. Mater.*, 1991, **3**, 225; (*c*) S. Hünig, *Pure Appl. Chem.*, 1990, **62**, 395.
3 R. Kato, H. Kobayashi, A. Kobayashi, T. Mori and H. Inokuchi, *Chem. Lett.*, 1987, 1579.
4 A. Kobayashi, R. Kato, H. Koabayashi, T. Mori and H. Inokuchi, *Solid State Commun.*, 1987, **64**, 45.
5 R. Kato, H. Kobayashi and A. Kobayashi, *J. Am. Chem. Soc.*, 1989, **111**, 5224.
6 S. Tomić, D. Jérome, A. Aumüller, P. Erk, S. Hünig and J. U. von Schütz, *J. Phys. C*, 1988, **21**, L203; S. Tomić, D. Jérome, A. Aumüller, P. Erk, S. Hünig and J. U. von Schütz, *Europhys. Lett.*, 1988, **5**, 553.
7 (*a*) I. H. Inoue, A. Kakizaki, H. Namatame, A. Fujimori, A. Kobayashi, R. Kato and H. Kobayashi, *Phys. Rev. B*, 1992, **45**, 5828; (*b*) H. Kobayashi, A. Miyamoto, R. Kato, F. Sakai, A. Kobayashi, Y. Yamakita, Y. Furukawa, M. Tasumi and T. Watanabe, *Phys. Rev. B*, 1993, **47**, 3500.
8 S. Uji, T. Terashima, H. Aoki, J. S. Brooks, R, Kato, H. Sawa, S. Aonuma, M. Tamura and M. Kinoshita, *Phys. Rev. B*, 1994, **50**, 15 597.
9 H. Kobayashi, R. Kato, A. Kobayashi, T. Mori and H. Inokuchi, *Solid State Commun.*, 1988, **65**, 1351.
10 R. Kato, H. Sawa, S. Aonuma, Y. Okano, S. Kagoshima, A. Kobayashi and H. Kobayashi, *Synth. Met.*, 1993, **55–47**, 1864.
11 (*a*) S. Hünig, K. Sinzger, M. Jopp, D. Bauer, W. Bietsch, J. U. von Schütz and H. C. Wolf, *Angew. Chem., Int. Ed. Engl.*, 1992, **31**, 859; (*b*) K. Sinzger, S. Hünig, M. Jopp, D. Bauer, W. Bietsch, J. U. von Schütz, H. C. Wolf, R. K. Kremer, T. Metzenthin, R. Bau, S. I. Khan, A. Lindbaum, C. L. Lengauer and E. Tillmanns, *J. Am. Chem. Soc.*, 1993, **115**, 7696.

12 G. Lunardi and C. Pecile, *J. Chem. Phys.*, 1991, **95**, 6911.

13 S. Aonuma, H. Sawa, Y. Okano, R. Kato and H. Kobayashi, *Synth. Met.*, 1993, **58**, 29.

14 R. A. Cox, *J. Phys. Org. Chem.*, 1991, **4**, 233.

15 H. L. Holland, F. M. Brown and M. Conn, *J. Chem. Soc., Perkin Trans. 2*, 1990, 1651.

16 R. Renaud and L. C. Leitch, *Can. J. Chem.*, 1956, **34**, 98.

17 H. Sawa, M. Tamura, S. Aonuma, M. Kinoshita and R. Kato, *J. Phys. Soc. Jpn.*, 1994, **63**, 4302.

18 R. Kato, H. Sawa, S. Aonuma, M. Tamura, M. Kinoshita and H. Kobayashi, *Solid State Commun.*, 1993, **85**, 831.

19 S. Aonuma, H. Sawa and R. Kato, *Chem. Lett.*, 1993, 513.

20 For review, see R. E. Carter and L. Melander, *Adv. Phys. Org. Chem.*, 1973, **10**, 1.

21 L. S. Bartell, K. Kuchitsu and R. J. deNeui, *J. Chem. Phys.*, 1961, **35**, 1211; L. S. Bartell and H. K. Higginbotham, *J. Chem. Phys.*, 1965, **42**, 851.

22 D. T. Cromer, R. R. Ryan and D. Schiferl, *J. Phys. Chem.*, 1985, **89**, 2315; D. Cavagnat, S. F. Trevino and A. Magerl, *J. Phys., Condens. Matter*, 1989, **1**, 10 047.

23 For review, see E. A. Halevi, *Prog. Phys. Org. Chem.*, 1963, **1**, 109.

24 K. A. Kobe and H. Levin, *Ind. Eng. Chem.*, 1950, **42**, 352.

Paper 4/06648K
Received 31*st October* 1994
Accepted 20*th February* 1995